Pol. J. Environ. Stud. Vol. 32, No. 2 (2023), 1199-1217
DOI: *10.15244/pjoes/156471* ONLINE PUBLICATION DATE: 2022-12-23

Original Research

Suitable Area of Invasive Species *Alexandrium* under Climate Change Scenarios in China Sea Areas

Ru Lan[1,2]*, Rongchang Chen[2], Hai Lin[1], Yi Huang[3], Rulin Wang[3,4]**

[1]University of Science and Technology Beijing, Beijing 100083, China
[2]China Waterborne Transport Research Institute, Beijing 100088, China
[3]Tibet University, Lhasa 850011, Tibet, China
[4]Sichuan Provincial Rural Economic Information Center, Chengdu 610072, Sichuan, China

Received: 12 October 2022
Accepted: 11 November 2022

Abstract

Alien invasive algae along with ship ballast water have posed a serious threat to China's marine ecological security. A clear understanding of the geographical distribution of invasive species and their response to climate change can provide a scientific basis for their prevention and control. In this study, combined with environmental variables and distribution data, MaxEnt was used to predict the potential geographical distribution and change trend of *Alexandrium* in the four major sea areas of China currently, 2040s (2040-2050) and 2090s (2090-2100), reveal the dominant environmental factors affecting the geographical distribution, analyze the migration trends of centroids the highly suitable area, and clarify the key control sea areas. The results showed that: 1) The AUC values of all models were significantly higher than random models, and the Kappa statistics of all models were higher than "general", demonstrated that the prediction results were available. 2) The most important environmental variable affecting the geographical distribution of *Alexandrium* was the Temperature. Range (bio24), and its suitable range was 23.43-31.52ºC. 2) At present, in the corresponding sea areas of Nantong, Yancheng, Ningbo, Jiaxing, Dongying, Binzhou, Cangzhou, Tianjin, Tangshan, Qinhuangdao, Shenzhen, Dongguan and Zhongshan, special attention should be paid to the control of *Alexandrium*. 3) Under the future climate change scenarios, excepted in the South China Sea, the total and highly suitable area of *Alexandrium* showed an increasing trend. 4) Under climate change scenarios, in the Yellow Sea, the centroids of the highly suitable area would move to the southeast. In the Bohai Sea and the East China Sea, the centroid showed a trend of moving to different latitudes and directions. In the South China Sea, the centroids of of the highly suitable area and total suitable area of *Alexandrium* would both

*e-mail: lanru@wti.ac.cn
**e-mail: linhai@ces.ustb.edu.cn

move to the southwest. Our results can provide a theoretical basis for the prevention and control of *Alexandrium*.

Keywords: *Alexandrium*, MaxEnt, climate change, suitable area

Introduction

The invasion of marine organisms has threatened the environmental and ecological safety of the ocean, and has been concerned by the world environmental organization [1, 2]. Ship ballast water and its sediments are considered to be one of the main carriers for the global transfer of aquatic organisms, including harmful aquatic organisms and pathogens [3-5]. The aquatic microorganisms, phytoplankton and aquatic animals contained in ballast water are discharged into the new ecosystem as the ship crosses the global ocean. The long-distance transfer of ballast water and sediment enables aquatic organisms to spread across natural biogeographic barriers, providing opportunities and possibilities for species invasion [6-8]. Thousands of species flow with ballast water around the world every day, among which more than 100 alien species have been identified by scientists as suspected alien species [9, 10]. After successful colonization in the new environment, alien species will multiply in large numbers and become dominant species, which may lead to repeated invasion disasters periodically.

Since the 1990s, China has begun to pay attention to and study the introduction of species into ballast water. Chu et al. collected 12 ballast water samples from five container ships entering Hong Kong from June 1994 to October 1995, and found at least 81 alien species from eight phyla of animals and five phyla of protozoa [11]. Wang et al. investigated the abundance and diversity of red tide forming species in ballast water during the study of species causing red tide in the ballast water of Yangshan Deepwater Port, and identified a total of 21 red tide forming species in 10 different sea areas [12]. Wu et al. measured the diversity and abundance of phytoplankton in the ballast water of 26 ships in Shanghai Yangshan deepwater port from April 2015 to January 2016, identified 84 species of phytoplankton, and found 9 potentially harmful phytoplankton [13].

Climate change has a great impact on species distribution and regional ecosystems [14, 15]. It is an effective means to determine the impact of climate change on the ecosystem by simulating the distribution of species through corresponding scientific means and determining the areas where sensitive species exist or may exist [16, 17]. Invasive plants have a great impact on many aspects of the ecological environment. In recent years, with the rapid development of marine transportation, many aquatic organisms, including harmful aquatic organisms and pathogens, have crossed the geographical barrier to China's sea area through ship ballast water [18, 19]. At present, marine biological invasion has been very serious, and has threatened the environmental and ecological security of China's marine environment. However, there are few reports on the dominant environmental factors and their thresholds that affect the geographical distribution of typical invasive algae in China at the macro level, so it is necessary to carry out such studies.

In this paper, we take *Alexandrium* as the research object, obtained its detailed geographical distribution records through field investigation, used ArcGIS software and MaxEnt model to predict its potential geographical distribution and changes in China's four major sea areas in different periods, and revealed the main environmental factors affecting its geographical distribution, so as to provide a theoretical basis for the prevention and control of *Alexandrium*.

Materials and Methods

Occurrence Data of Species

Occurrence data of *Alexandrium* were collected through the field survey of Chinese wharves from 2017 to 2022 and the environmental impact assessment report of the water transport Research Institute of the Ministry of Transport of China from 2012 to 2022. Firstly, Microsoft Excel (2010) was used to remove duplicate records. Second, the distance between each point and the center of the cell grid was calculated, and the point closest to the center in each cell grid was retained. After the above procedures, 94 distribution points of *Alexandrium* were retained for the establishment of MaxEnt (Table S1).

Environmental Data

Data of environmental variables were from Bio-OR ICLE environmental database of global marine biological diffusion model (http://bio-oracle.org). The climate data of current and future (RCP8.5, RCP4.5, RCP6.0 and RCP2.6) emission scenarios were downloaded respectively, with a spatial resolution of 5 arcmin (about 9.2 km^2). Twenty four environmental variables affecting the distribution of marine algae were selected (Table 1).

Modelling Process

MaxEnt software operation procedure was as follows. 1) The occurrence data of *Alexandrium* in "CSV" format and the environmental variable in "ASC" format were imported into the "sample" and "environmental layers" data boxes of MaxEnt

Table 1. Marine hydrological environmental variables.

Number	Environmental variables	Parameter
1	bio1	Currents velocity. Lt. max
2	bio2	Currents velocity. Lt. min
3	bio3	Currents velocity. max
4	bio4	Currents velocity. mean
5	bio5	Currents velocity. min
6	bio6	Currents velocity. range
7	bio7	Ice thickness. Lt. max
8	bio8	Ice thickness. Lt. min
9	bio9	Ice thickness.max
10	bio10	Ice thickness.mean
11	bio11	Ice thickness.min
12	bio12	Ice thickness. range
13	bio13	Salinity. Lt. max
14	bio14	Salinity. Lt. min
15	bio15	Salinity. max
16	bio16	Salinity. mean
17	bio17	Salinity. min
18	bio18	Salinity. range
19	bio19	Temperature. Lt. max
20	bio20	Temperature. Lt. min
21	bio21	Temperature. max
22	bio22	Temperature. mean
23	bio23	Temperature. min
24	bio24	Temperature. Range

software (V3.4.4) respectively. 2) "Create response curves" and "Do jackknife to measure variable importance" were selected respectively to analyze the relationship between variables and presence probability of *E. granulosus* and measure the importance of variables. 3) In the initial model, "Random test percentage" was set to 25 %, while in the reconstructed model, "random seed" was selected, and the "replicates" was set to 10 [20, 21].

Evaluation of MaxEnt

Receiver operating characteristic (ROC) is a highly recognized diagnostic test evaluation index, and the value range of area value under ROC curve, i.e. AUC value, is 0.5-1 [22]. Kappa statistics is a consistency test method, which comprehensively considers the species distribution rate, sensitivity and specificity, and is widely used in model evaluation. The value range of Kappa is -1–1. When Kappa is greater than 0.75, it means good consistency, and less than 0.4 means poor consistency [21, 23].

Results and Discussion

Selection of Modeling Variables

In order to avoid multi-collinearity among 24 environmental variables, Pearson correlation analysis method was used. Firstly, MaxEnt was used to calculate the percent contributions of 24 variables, and the variable whose percent contribution rate was greater than 0 were retained (Table S2). Thereafter, the Pearson's coefficients between two variables with percent contribution greater than 0 corresponding to 94 occurrence data of *Alexandrium* were analyzed using SPSS. Thirdly, by comparing the percentage contribution of the variables with the absolute value of the coefficient greater than 0.85 (Table S3), the higher one was retained. Finally, 7 variables of Currents Velocity Range (bio6), Ice Thickness. Mean (bio10), Salinity. Lt. Max (bio13), Salinity. Min(bio17), Salinity. Range (bio18), Temperature. Lt. Max (bio19) and Temperature. Range (bio24) were retained to establish the prediction model of *Alexandrium*.

Model Performance

In this paper, 10 groups of repetitions were used to test the AUC values and Kappa consistency of the models. The AUC values under the current situation was 0.975±0.001. In 2040s, the AUC values of RCP2.6, RCP4.5, RCP6.0 and RCP8.5 scenarios were 0.975±0.001, 0.975±0.002, 0.976±0.001 and 0.977±0.001, respectively. In 2090s, the AUC values of RCP2.6, RCP4.5, RCP6.0 and RCP8.5 scenarios were 0.975±0.001, 0.976±0.002, 0.977±0.001 and 0.973±0.003, respectively. The above showed that the AUC values of all models were significantly higher than random models, and they all achieved high accuracy.

The Kappa statistics under the current situation was 0.745±0.072. In 2040s, the Kappa values of RCP2.6, RCP4.5, RCP6.0 and RCP8.5 scenarios were 0.755±0.085, 0.688±0.081, 0.759±0.079 and 0.756±0.082, respectively. In 2090s, the AUC values of RCP2.6, RCP4.5, RCP6.0 and RCP8.5 scenarios were 0.698±0.087, 0.743±0.071, 0.648±0.102 and 0.734±0.079, respectively. The above showed that the Kappa statistics of all models were higher than "general", and the prediction results were available.

Dominant Variables

Percent Contribution and Permutation Importance of Variables

The percent contribution and permutation importance of modeling variables can be measured by

Table 2. The AUC and Kappa values of the three models.

	AUC	Kappa
Current	0.975±0.001	0.745±0.072
2040s, RCP2.6	0.975±0.001	0.755±0.085
2040s, RCP4.5	0.977±0.002	0.688±0.081
2040s, RCP6.0	0.976±0.001	0.759±0.079
2040s, RCP8.5	0.977±0.001	0.756±0.082
2090s, RCP2.6	0.975±0.001	0.698±0.087
2090s, RCP4.5	0.976±0.001	0.743±0.071
2090s, RCP6.0	0.977±0.002	0.648±0.102
2090s, RCP8.5	0.974±0.003	0.734±0.079

MaxEnt's own module. Results showed that (Fig. 1), the percent contribution rate of Temperature. Range (bio24) was the highest (73.34 %), and the remaining variables were ranked as Salinity. Range (bio18, 11.76%), Ice Thickness. Mean (bio10, 7.01%), Temperature. Lt. Max (bio23, 3.79%), Salinity. Lt. Max (bio15, 2.73%), (bio2, 0.94%), (bio1, 0.33) and Currents Velocity. Range (bio5, 0.1%).

In terms of permutation importance, Temperature. Lt. Max (bio19) was the highest (94.87%), followed by Temperature. Range (bio24, 3.97%), while the permutation importance of the remaining variables was less than 1%.

Jackknife Test of Variables

Results of Jackknife test (Fig. 2) showed that when modeling with a single variable, the regularized training gain of Temperature. Range (bio24) was the highest (4.1), indicating its importance to modeling. When Salinity. Min (bio17), Salinity. Lt. Max (bio13) and Salinity. Range (bio18) were used for modeling alone, their regularized training scores exceeded 2. These

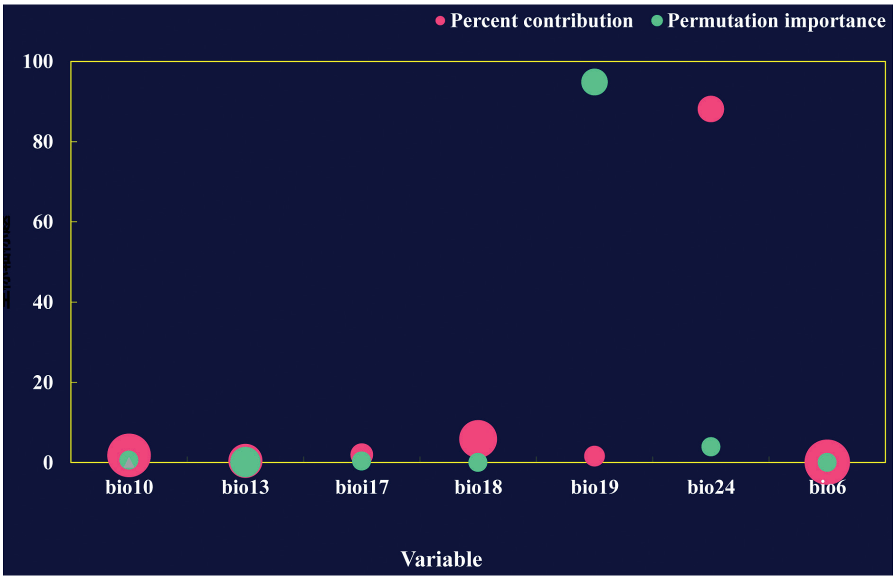

Fig. 1. Percent contribution and permutation importance of variables.

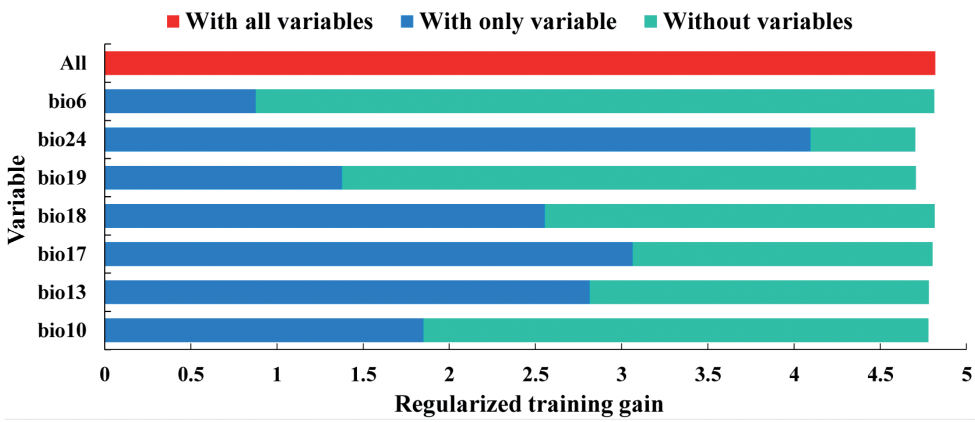

Fig. 2. Jackknife test of seven variables.

indicated that the above variables play a dominant role in restricting the geographical distribution of *Alexandrium*.

Response Curves of Variables

According to the percent contribution rate and permutation importance of environmental variables, combined with the Jackknife test, the dominant variables affecting the distribution of *Alexandrium* were selected, and the response curves were drawn (Fig. 3). The response curve can be used to judge the value of environmental variables that are beneficial or detrimental to the growth of *Alexandrium*. In this study, taking the presence probability of 0.5 as the threshold.

With the increase of Temperature. Range (bio24), the presence probability of *Alexandrium* showed an upward trend and reached 0.5 at 24.62ºC, and reached the maximum (0.97) at 27.61ºC. When Temperature. Range (bio24) reached 31.52ºC, the presence probability of *Alexandrium* decreased slightly, but it was greater than 0.83. Therefore, the range of Temperature. Range suitable (bio24) for *Alexandrium* growth was 23.43-31.52ºC (Fig. 3a).

With the increase of Temperature. Lt. Max (bio19), the presence probability of *Alexandrium* showed an upward trend and reached 0.5 at 15.32ºC, and reached the peak (0.93) at 26.57ºC. With the continuous increase of Temperature. Lt. Max (bio19) to 27.6ºC, the presence probability decreased to 0.5, so the range of Temperature. Lt. Max (bio19) suitable for *Alexandrium* growth was 15.32-27.6ºC (Fig. 3b).

With the increase of Salinity. Min (bio17), the presence probability of *Alexandrium* showed an upward trend and reached 0.5 at 8.59%, and reached the peak (0.99) at 12.72 %. With the continuous increase of Salinity. Min (bio17) to 19.17%, the presence probability decreased to 0.5, so the range of Salinity. Min (bio17) suitable for *Alexandrium* growth was 8.59%-19.17% (Fig. 3c).

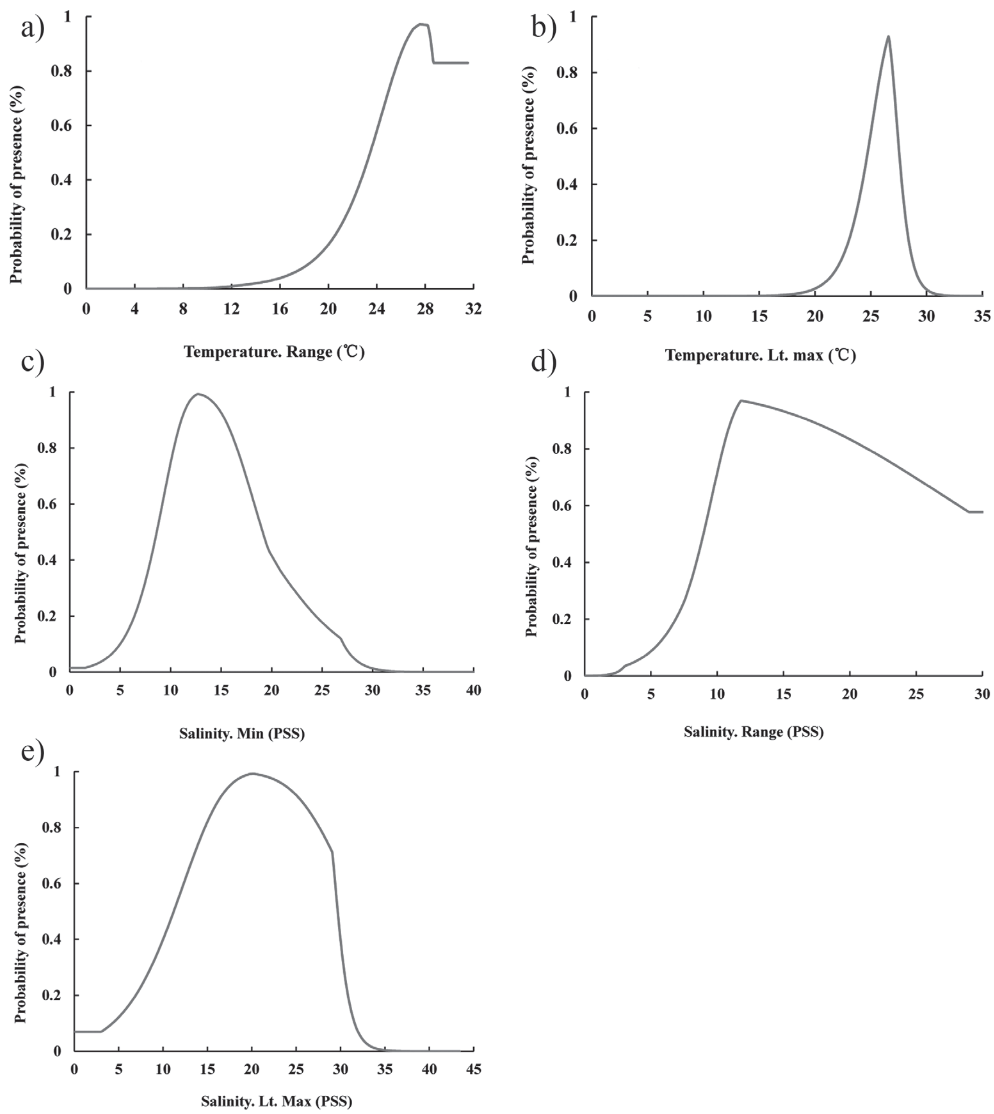

Fig. 3. Response curves of key variables.

With the increase of Salinity. Range (bio18), the presence probability of *Alexandrium* showed an upward trend and reached 0.5 at 8.96%, and reached the maximum (0.97) at 11.86%. When Salinity. Range (bio18) reached 31.85%, the presence probability of *Alexandrium* decreased slightly, but it was greater than 0.58. Therefore, the range of Salinity. Range (bio18) suitable (bio24) for *Alexandrium* growth was 8.96%-31.85 % (Fig. 3d).

With the increase of Salinity. Lt. Max (bio13), the presence probability of *Alexandrium* showed an upward trend and reached 0.5 at 11.17%, and reached the peak (0.99) at 20.16%. With the continuous increase of Salinity. Lt. Max (bio13) to 29.68%, the presence probability decreased to 0.5, so the range of Salinity. Lt. Max (bio13) suitable for *Alexandrium* growth was 11.17%-29.68 (Fig. 3e).

In limiting the potential distribution of species, climate factors are the key factors on the macro scale, and the study of the interaction between plants and climate is an important direction of ecology [24-26]. In this study, the important analysis showed that the top two environmental variables in percent contribution rate were Temperature. range (bio24) and Temperature. Lt. Max (bio19). Zhao et al. showed by exploring the relationship between *Alexandrium* and environmental factors that when the temperature was higher or lower than a certain temperature, its growth would be limited [27]. You explored the response of growth to important environmental factors and showed that the growth of *Alexandrium* was mainly limited by temperature [28]. Similar laws have been found in the study of other algae. Li et al. showed that temperature is the dominant environmental factor limiting the suitability of *Macrocystis pyrifera* in China [29]. Li et al. showed that the appropriate temperature was crucial for the growth of *Costaria costata* [30]. Norma et al. explored the potential distribution of invasive freshwater *Ceratium furcoides* in South America and found that its suitable habitat would change with the increase of temperature [31].

In addition to temperature variables, Salinity. Min (bio17), Salinity. Range (bio18) and Salinity. Lt. Max (bio13) also affected the distribution of *Alexandrium*. Response curve showed that when the salinity was too high or too low to a certain extent, it would exceed the threshold suitable for *Alexandrium*, which would reduce its survival probability in some areas. Zhao et al. also proved the key of salinity to the growth restriction of *Alexandrium* by exploring the relationship between *Alexandrium* and environmental factors [27].

Potential Geographical Distribution of *Alexandrium* in Bohai Sea, Yellow Sea, East China Sea and South China Sea

Potential Geographical Distribution under Current Situation

In the Bohai Sea, *Alexandrium* was suitable in most areas, with a total suitable area of 8.62 × 10^4 km^2. The area of the highly suitable area accounts for 48.47% of the total suitable area, with an area of 4.18 × 10^4, part of which was distributed in the sea areas corresponding to Dongying, Binzhou, Cangzhou,

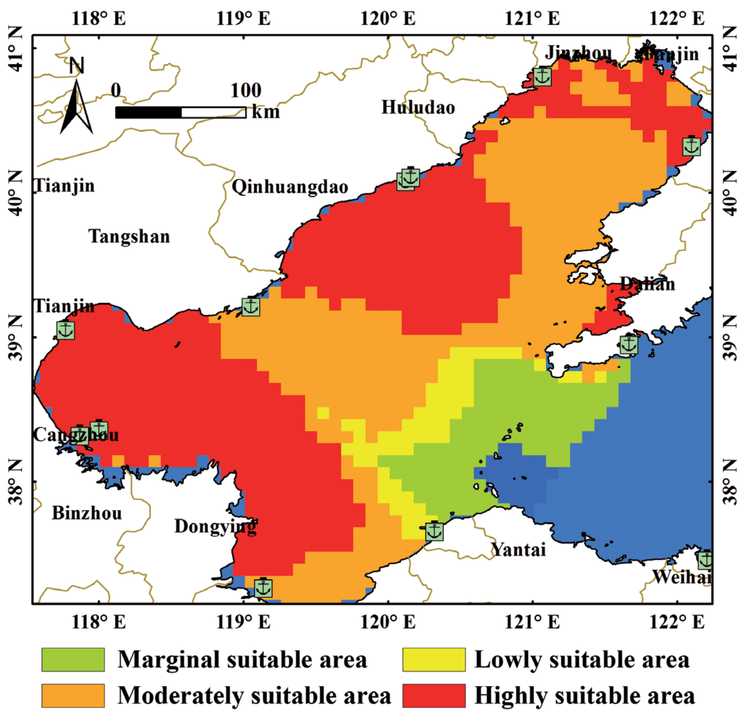

Fig. 4. Potential suitable area in the Bohai Sea under current situation.

Tianjin and Tangshan, the other part was distributed in the sea areas corresponding to Qinhuangdao in a pie shape, and the other part was distributed in the sea areas corresponding to Dalian, Yingkou, Jinzhou and Panjin in a scattered shape. The area of moderately suitable area was 3.12 × 10^4 km^2, accounting for 36.23% of the total suitable area, mainly distributed in the corresponding sea areas of Dalian, Tangshan and Weifang. The area of the lowly suitable area was 0.45 × 10^4 km^2, accounting for 5.23% of the total suitable area, surrounded by thin strips in the periphery of the moderately suitable area. The marginal suitable area accounts for 10.06% of the total suitable area, with an area of 0.87 × 10^4 km^2, extending to the open sea next to the lowly suitable area. In general, most of the Bohai Sea was suitable for *Alexandrium*, and the highly and moderately suitable areas account for 84.70% of the total suitable areas. Therefore, special attention should be paid to the prevention and control of *Alexandrium* in the sea areas corresponding to the cities along the Bohai Sea (Fig. 4).

In the Yellow Sea, *Alexandrium* was mainly distributed in the corresponding sea areas of Nantong, Yancheng, Lianyungang, Rizhao, Qingdao, Weihai and Yantai, with a total area of 25.67 × 10^4 km^2. The area of the highly suitable area accounted for 9.58% of the total suitable area, with an area of 2.46 × 10^4 km^2, mainly distributed in strips in the sea areas corresponding to Nantong and Yancheng. The area of the moderately suitable area accounted for 7.96% of the total suitable area, with an area of 2.04 × 10^4 km^2, mainly surrounded by strips in the periphery of the highly suitable area, and the other part was dotted in the corresponding sea areas of Lianyungang and Rizhao. The area of the lowly suitable area accounted for 21.79% of the total suitable area, with an area of 5.59 × 10^4 km^2, mainly surrounded by strips in the periphery of the moderately suitable area. The marginal suitable area accounted for 60.67% of the total suitable area, with an area of 15.57 × 10^4 km^2, distributed in the corresponding sea area from Nantong to Yantai. In general, the corresponding waters of Nantong and Yancheng need to pay attention to the prevention and control of *Alexandrium* (Fig. 5).

In the East China Sea, *Alexandrium* was mainly distributed in the corresponding sea areas of Quanzhou, Putian, Fuzhou, Ningde, Wenzhou, Taizhou, Zhoushan, Jiaxing and Shanghai, with a total area of 10.9 × 10^4 km^2. The area of the highly suitable area accounted for 16.15% of the total suitable area, with an area of 1.76 × 10^4 km^2, mainly distributed the corresponding sea areas of Ningbo and Jiaxing. The area of the moderately suitable area accounted for 11.8% of the total suitable area, with an area of 1.29 × 10^4 km^2, one part was distributed in strips in the sea areas of Shanghai and Jiaxing, and the other part was distributed in strips in the sea areas outside the highly suitable area. The area of the lowly suitable area accounted for 22.31% of the total suitable area, with an area of 2.43 × 10^4 km^2, mainly surrounded by strips around the periphery of the moderately suitable area, and another small part was distributed in dots. The marginal suitable area accounted for 49.71% of the total suitable area. From Taizhou to Shanghai, it was distributed in the periphery of the lowly suitable area, while from Wenzhou to Quanzhou, it was distributed along the coast. In general, the corresponding sea areas of Ningbo and Shanghai

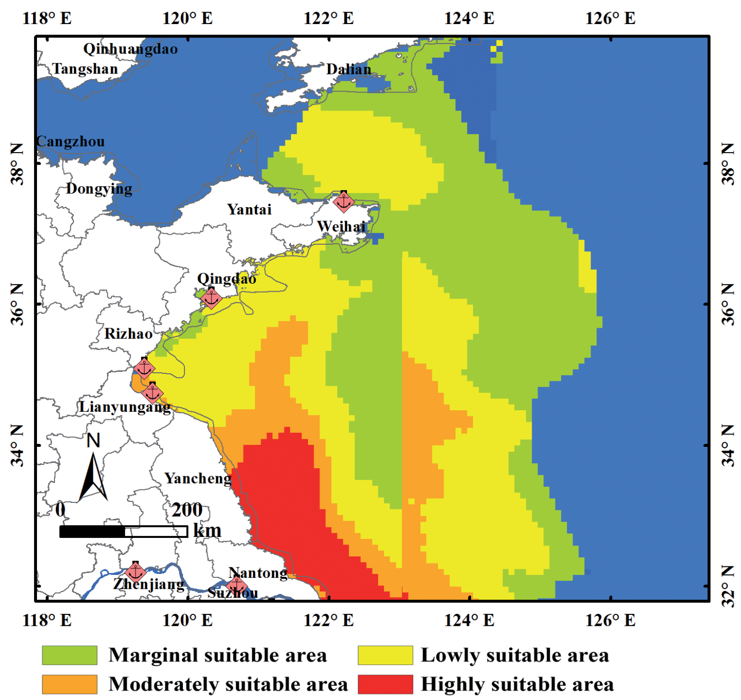

Fig. 5. Potential suitable area in the Yellow Sea under current situation.

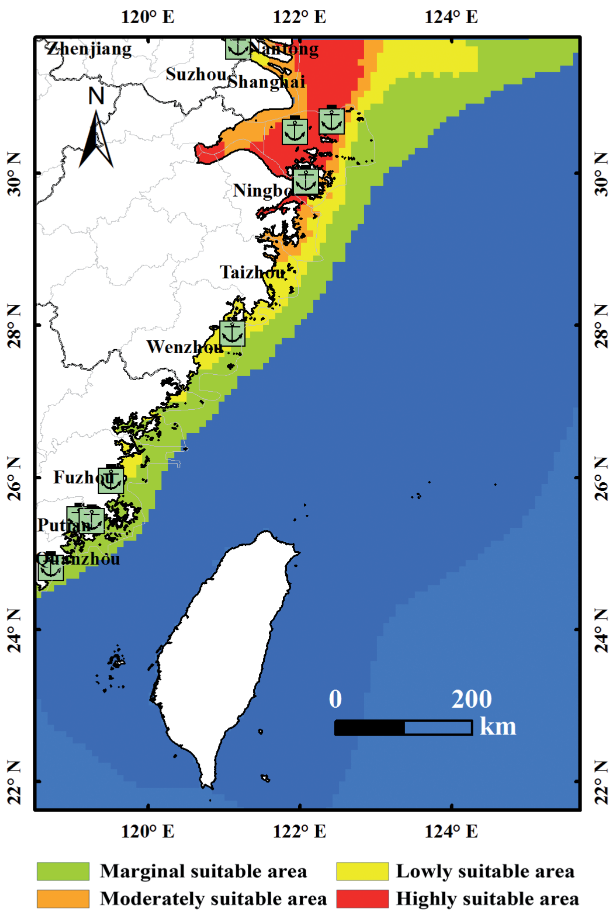

Fig. 6. Potential suitable area in the East China Sea under current situation.

need to pay attention to the prevention and control of *Alexandrium* (Fig. 6).

In the South China Sea, *Alexandrium* was dominated by marginal suitable areas, and the areas of the highly suitable area,moderately suitable area and lowly suitable areas were very small, with a total area of 5.22×10^4 km^2. The area of the highly suitable area accounted for 3.83% of the total suitable area, with an area of 0.2×10^4 km^2, mainly distributed the corresponding sea areas of Shenzhen, Dongguan and Zhongshan. The area of the moderately suitable area accounted for 3.17% of the total suitable area, with an area of 0.17×10^4 km^2, one part was strip-shaped surrounding the periphery of the highly suitable area, and the other part was dotted in the sea area corresponding to Jiangmen. The area of the lowly suitable area accounted for 10.3% of the total suitable area, with an area of 0.64×10^4 km^2, mainly in thin strips surrounding the periphery of the moderately suitable area. The marginal suitable area accounted for 82.69% of the total suitable area, with an area of 4.32×10^4 km^{2,} distributed in thin strips in the corresponding sea area from Zhanjiang to Zhangzhou. In general, most of the sea areas in the South China Sea were not suitable for the survival of *Alexandrium*, and the low suitable areas and marginal suitable areas accounted for 84.70% of the total suitable areas. Therefore, we only need to pay attention to the prevention and control of *Alexandrium* in the corresponding sea areas of Shenzhen, Dongguan and Zhongshan (Fig. 7).

In the past few decades, the research on global climate and environmental change has attracted more

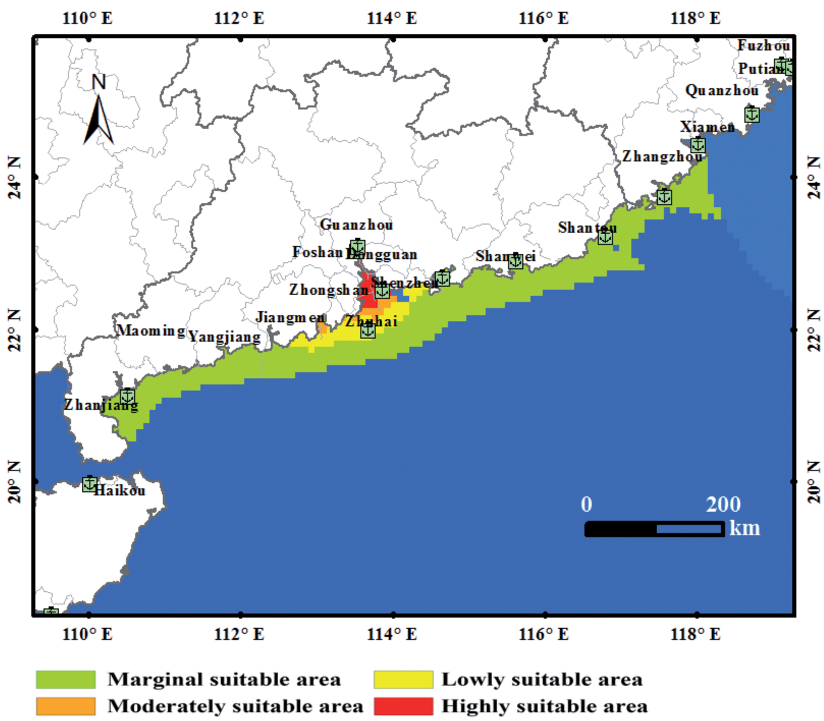

Fig. 7. Potential suitable area in the South China Sea under current situation.

and more attention in the field of scientific research [32, 33]. Many scholars have carried out research on the suitable areas of invasive plants [34, 35]. Sayit et al. explored the distribution pattern of invasive plant *Xanthium spinosum* [36], Chen et al. explored the proliferation risk of invasive plant *Tithonia diversifolia* [37], Li et al. predicted the distribution area of *Flaveria bidentis* [38]. In this study, MaxEnt was used to analyze the potential distribution areas of *Alexandrium* in the Bohai Sea, the Yellow Sea, the East China Sea and the South China Sea. Results showed that *Alexandrium* was distributed in most areas of the Bohai Sea, the corresponding sea areas of Nantong and Yancheng in the Yellow sea, the corresponding sea areas of Ningbo and Jiaxing in the East China sea, the corresponding sea areas of Shenzhen, Dongguan and Zhongshan in the South China sea. According to the actual investigation, the occurrence frequency of *Alexandrium* in each sea area is basically consistent with the simulation results, which confirms the accuracy. In the above-mentioned high fitness areas, a situation should be formed in which prevention is the primary and treatment is the secondary. For the prevention and control of *Alexandrium*, scientific research institutions should actively explore the research of biological agents, such as using fungi, bacteria, viruses or native algae to inhibit the growth of *Alexandrium* [39]. Administrative units need to actively promote the prevention and control of *Alexandrium* in management, and should also take corresponding measures in the input link as far as possible. First of all, we should actively promote the publicity and education of *Alexandrium* prevention and control, improve the national awareness of prevention and control, and encourage ships to prevent and control by themselves [40]. Secondly, the key sea areas should be monitored and ready for prevention and control at any time. Third, effective prevention and control technologies should be actively promoted. Finally, for ships that bring *Alexandrium* and cause serious consequences, in addition to increasing the punishment, they should also be prohibited from berthing again [41, 42].

Potential Geographical Distribution under Climate Change Scenarios

Compared with the current distribution, under RCP2.6, RCP4.5, RCP6.0 and RCP8.5 in the 2040s, the total suitable area of *Alexandrium* in the Bohai Sea would increase by 2.01%, 0.64%, 1.85% and 2.01% respectively, the area of the highly suitable area would increase by 40.20%, 51.33%, 71.26% and 9.14% respectively, the area of the moderately suitable area would decrease by 33.56%, 50.44%, 72.00% and 12.67% respectively, and the area of the marginal suitable area would decrease by 46.40%, 59.20%, 64.00% and 74.40% respectively. Under RCP8.5, the area of the poorly suitable area would increase by 184.62%, remain unchanged under RCP4.5, reduce by 12.31% and 4.62% respectively under RCP2.6 and RCP6.0 (Fig. 8A-D).

Compared with the current distribution, under RCP2.6, RCP4.5, RCP6.0 and RCP8.5 in the 2090s, the total suitable area would increase by 0.32%, 2.01%, 2.01% and 2.01% respectively, the area of the highly suitable area would increase by 63.95%, 42.36%, 35.05% and 65.45% respectively, the area of the moderately suitable area would decrease by 62.89%, 35.78%, 27.78% and 63.11% respectively, while the area of marginal suitable area would decrease by 50.40%, 80.00%, 66.40% and 55.20% respectively. Under RCP2.6 and RCP8.5, the area of the poorly suitable area would be reduced by 53.85% and 24.62% respectively, while under RCP4.5 and RCP6.0, it would increase by 47.69% and 33.85% respectively (Fig. 8E-H).

Compared with the current distribution, under RCP2.6, RCP4.5, RCP6.0 and RCP8.5 in the 2040s, the

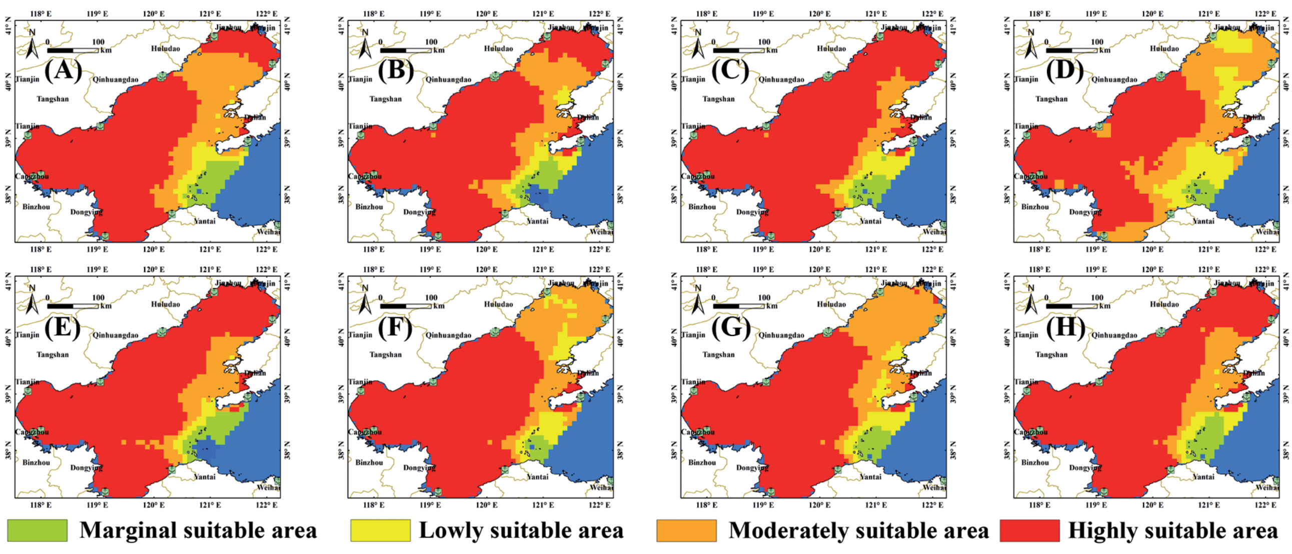

Fig. 8. Potential suitable area in the Bohai Sea under climate change scenarios.

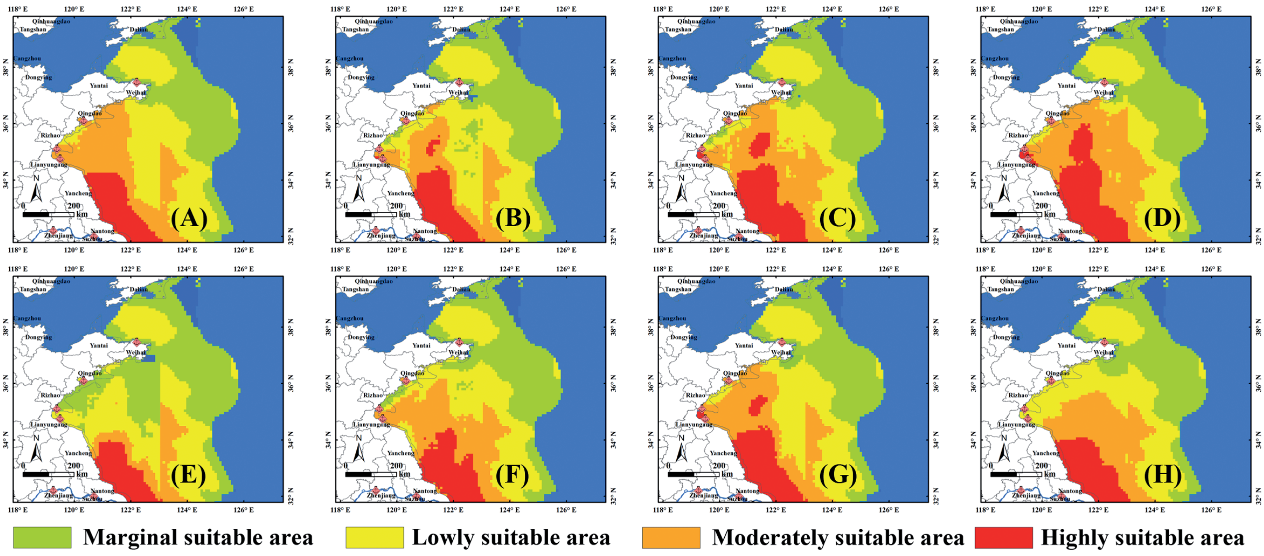

Fig. 9. Potential suitable area in the Yellow Sea under climate change scenarios.

total suitable area of *Alexandrium* in the Yellow Sea would increase by 14.35%, 21.09%, 24.23% and 25.09% respectively, the area of the highly suitable area would increase by 140.4%, 29.10%, 84.75% and 105.93% respectively, the area of the moderately suitable area would increase by 652.72%, 75.51%, 371.77% and 536.39% respectively, the area of the poorly suitable area would increase by 27.20%, 74.29%, 98.76% and 117.02% respectively, and the marginal suitable area would be reduced by 93.93%, 6.43%, 57.70% and 87.77% respectively (Fig. 9A-D).

Under RCP2.6, RCP4.5, RCP6.0 and RCP8.5 in the 2090s, the total suitable area would increase by 21.79%, 23.77%, 22.50% and 21.98% respectively, the area of the

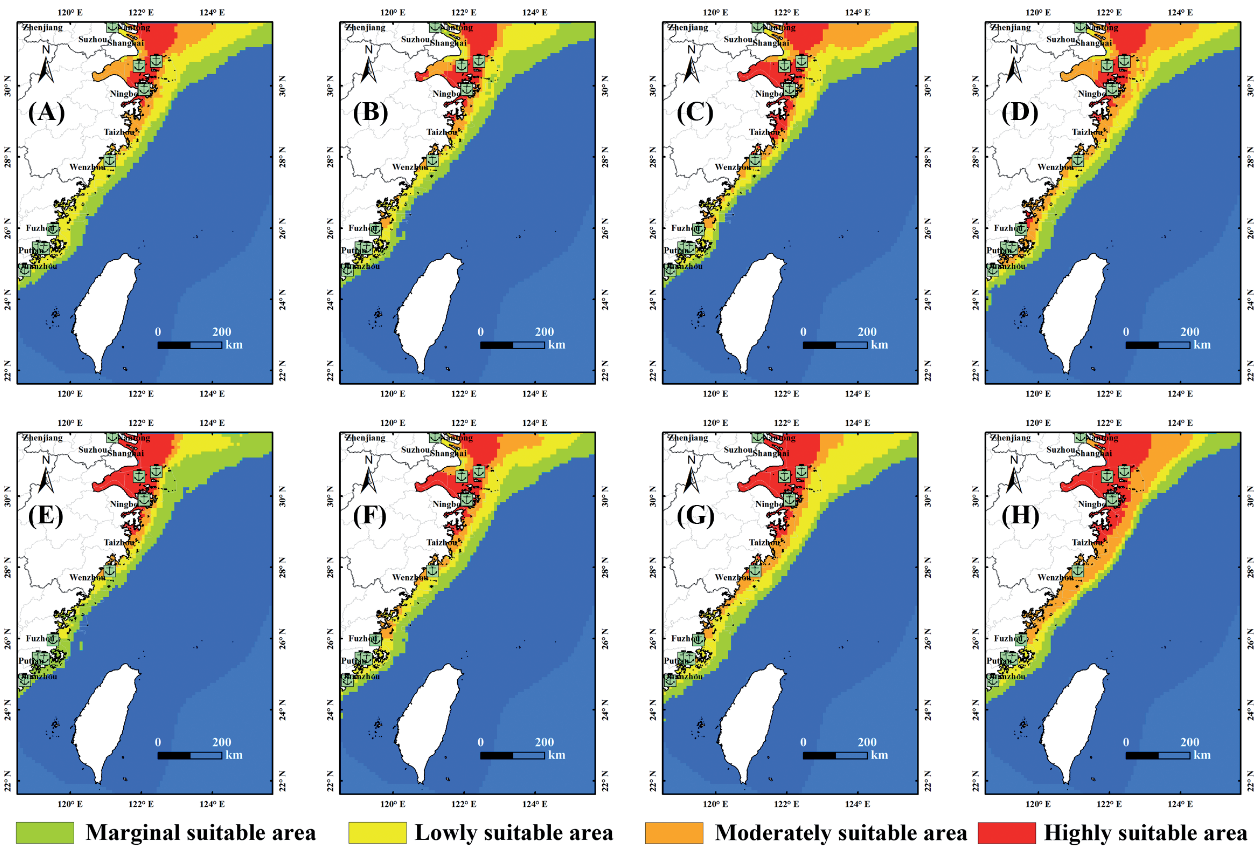

Fig. 10. Potential suitable area in the East China Sea under climate change scenarios.

highly suitable area would increase by 0.56%, 37.01%, 47.74% and 29.66% respectively, and the area of the poorly suitable area would increase by 4.22%, 168.45%, 182.36% and 80.62% respectively. Under RCP2.6, the area of the moderately suitable area would be reduced by 35.71%, and under other emission scenarios, it would increase by 270.07% (RCP4.5), 142.86% (RCP6.0) and 313.95% (RCP8.5) respectively. Under RCP2.6, the area of marginal suitable area would increase by 47.93%, and under other emission scenarios, it would decrease by 62.61% (RCP4.5), 54.71% (RCP6.0) and 38.60% (RCP8.5) respectively (Fig. 9E-H).

Compared with the current distribution, under RCP2.6, RCP4.5, RCP6.0 and RCP8.5 in the 2040s, the total suitable area of *Alexandrium* in the East China Sea would increase by 15.32%, 2.80%, 8.33% and 20.66% respectively, the moderately suitable area would increase by 98.92%, 38.71%, 123.66% and 241.94% respectively, the poorly suitable area would increase by 27.20%, 74.29%, 98.76% and 117.02% respectively, and the marginal suitable area would decrease by 96.01%, 43.59%, 37.04% and 36.47% respectively. Under RCP2.6, the area of the highly suitable area would be reduced by 12.20%, and under other emission scenarios, it would increase by 4.72% (RCP4.5), 36.61% (RCP6.0) and 3.15% (RCP8.5) respectively (Fig. 10A-D).

Under RCP2.6, RCP4.5, RCP6.0 and RCP8.5 in the 2090s, the total suitable area would increase by 1.40%, 12.65%, 24.03% and 21.98% respectively, the area of the highly suitable area would increase by 53.94%, 31.50%, 72.05% and 92.13% respectively, and the area of the marginal suitable area would decrease by 5.88%, 29.03%, 37.85% and 47.57% respectively. Under RCP2.6, the area of the moderately suitable area would be reduced by 25.81%, and under other emission scenarios, it would increase by 96.24% (RCP4.5), 84.41% (RCP6.0) and 213.98% (RCP8.5) respectively. Under RCP2.6 and RCP8.5, the area of the poorly suitable area would decrease by 5.98% and 22.79%, and increase by 95.16% and 47.58% under RCP4.5 and RCP6.0 (Fig. 10E-H).

Compared with the current distribution, under RCP2.6, RCP4.5, RCP6.0 and RCP8.5 in the 2040s, the total suitable area of *Alexandrium* in South China sea would be reduced by 21.00%, 37.65%, 45.97% and 21.00% respectively, the moderately suitable area would be increased by 179.17%, 154.17%, 145.83% and 216.67% respectively, the lowly suitable area would be increased by 88.46%, 17.95%, 34.62% and 93.59% respectively, and the marginal suitable area would be reduced by 39.62%, 57.51%, 67.09% and 47.44% respectively (Fig. 11A-D).

Under RCP2.6, the area of the highly suitable area would decrease by 79.31%, while under other emission scenarios, it would increase by 82.76%, 34.48% and 44.83% respectively.

Under RCP2.6, RCP4.5, RCP6.0 and RCP8.5 in the 2090s, the area of the total suitable area would be reduced by 34.61%, 25.36%, 1.06% and 14.00% respectively, the area of the highly suitable area would be increased by 155.17%, 96.55%, 337.93% and 234.48% respectively, the area of the moderately suitable area would be increased by 112.50%, 183.33%, 362.50% and 454.17% respectively, the area of the lowly suitable area would be increased by 17.95%, 66.67%, 103.85% and 58.97% respectively, and the area of the marginal suitable area would be reduced by 55.59%, 50.48%, 43.77% and 52.56% respectively (Fig. 11E-H).

Lambers et al. found that under the background of climate warming, some species would be extinct, but the distribution area of a large number of species would expand, which showed that climate warming is a double-edged sword for the growth and distribution of species [43]. Obviously, this study showed that climate warming would be conducive to the growth of *Alexandrium*, and its suitable habitat would be expanded in the sea

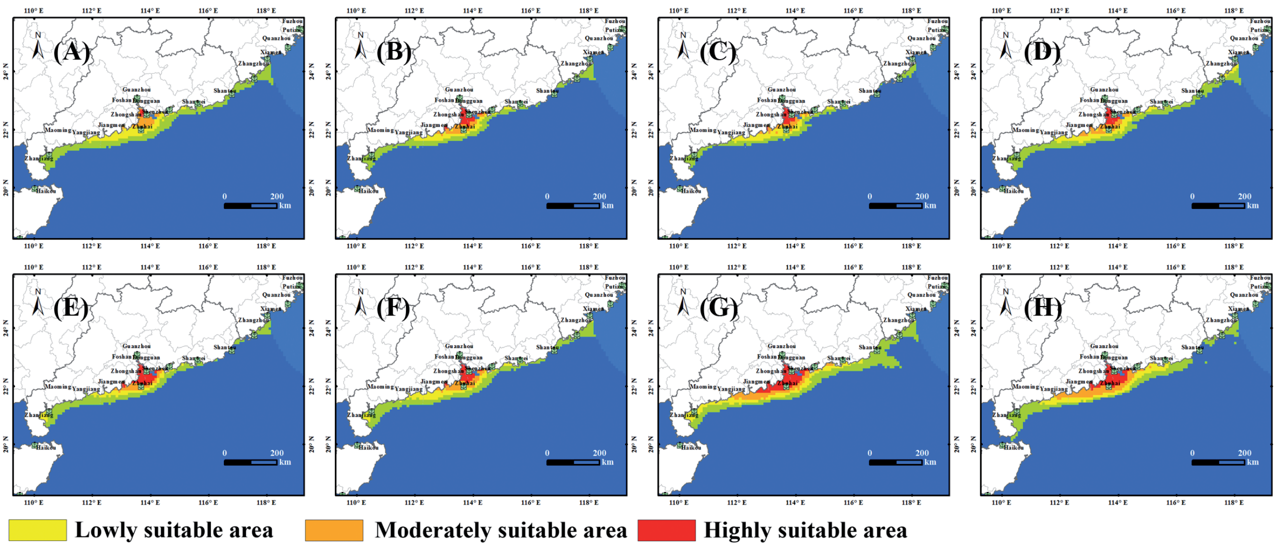

Fig. 11. Potential suitable area in the South China Sea under climate change scenarios.

areas of China. Climate change may accelerate and some species form new physiological characteristics to adapt [39, 44, 45]. Relevant studies have shown that changes in the temporal and spatial pattern of climate may lead to changes in the geographical distribution pattern of plants [20-22, 46]. Systematic exploration of the geographical distribution pattern of *Alexandrium* under the background of climate change can provide a scientific basis for prevention and control and the formulation of relevant prevention and control policies.

Trajectory Trend of Centroid of the Highly Suitable Habitat

Based on the centroid of the highly suitable habitat under the current and future climate change scenarios, the movement trajectory in the Bohai Sea was revealed as follows. 1) Under RCP2.6, the centroid would move from 119.53°E/ 39.07°N (current) to the southeast by 19.95 km to 119.57°E/38.88°N (2040s), and then to the northeast by 24.91 km to 119.78°E/39°N (2090s). From current to 2090s, the centroid would generally moved 27.38 km to the southeast (Fig. 12). 2) Under RCP4.5, the centroid would move from 119.53°E/ 39.07°N (current) to the southeast by 21.95 km to 119.69°E/38.93°N (2040s), and then to the southwest by 30.01 km to 119.52°E/38.69°N (2090s). From current to 2090s, the centroid would generally moved 38.17 km to the southwest (Fig. 12). 3) Under RCP6.0, the centroid would move from 119.53°E/ 39.07°N (current) to the southeast by 31.91 km to 119.84°E/39.01°N (2040s), and then to the southwest by 51.61 km to 119.45°E/38.67°N (2090s). From current to 2090s, the centroid would generally moved 40.96 km to the southwest (Fig. 12). 4) Under SSP5-8.5, the centroid would move from 119.53°E/ 39.07°N (current) to the southwest by 27.89 km to 119.37°E/38.84°N (2040s) , and then to the northeast by 44.22 km to 119.78°E/39°N (2090s). From current to 2090s, the centroid would generally moved 26.57 km to the southeast (Fig. 12).

Based on the centroid of the highly suitable habitat under the current and future climate change scenarios, the movement trajectory in the Yellow Sea was revealed as follows. 1) Under RCP2.6, the centroid would move from 121.57°E/ 32.94°N (current) to the northwest by 6.32 km to 121.56°E/33°N (2040s), and then to the sooutheast by 22.74 km to 121.69°E/32.81°N (2090s). From current to 2090s, the centroid would generally moved 17.39 km to the southeast (Fig. 13). 2) Under RCP4.5, the centroid would move from 121.57°E/ 32.94°N (current) to the northeast by 17.15 km to 121.58°E/33.11°N (2040s), and then to the southeast by 38.37 km to 121.91°E/32.89°N (2090s). From current to 2090s, the centroid would generally moved 34.21 km to the southeast (Fig. 13). 3) Under RCP6.0, the centroid would move from 121.57°E/ 32.94°N (current) to the northeast by 37.62 km to 121.77°E/33.25°N (2040s), and then to the southwest by 18.97 km to 121.59°E/33.21°N (2090s). From current to 2090s, the centroid would generally moved 27.91 km to the northeast (Fig. 13). 4) Under SSP5-8.5, the centroid would move from 121.57°E/ 32.94°N (current) to the northeas by 58.12 km to 119.37°E/38.84°N (2040s) , and then to the southeast by 63.07 km to 119.78°E/39°N (2090s). From current to 2090s, the centroid would generally moved 18.34 km to the southeast (Fig. 13).

Based on the centroid of the highly suitable habitat under the current and future climate change scenarios, the movement trajectory in the East China Sea was revealed as follows. 1) Under RCP2.6, the centroid would move from 122.03°E/30.69°N (current) to the northeast by 23.56 km to 122.22°E/30.84°N (2040s), and

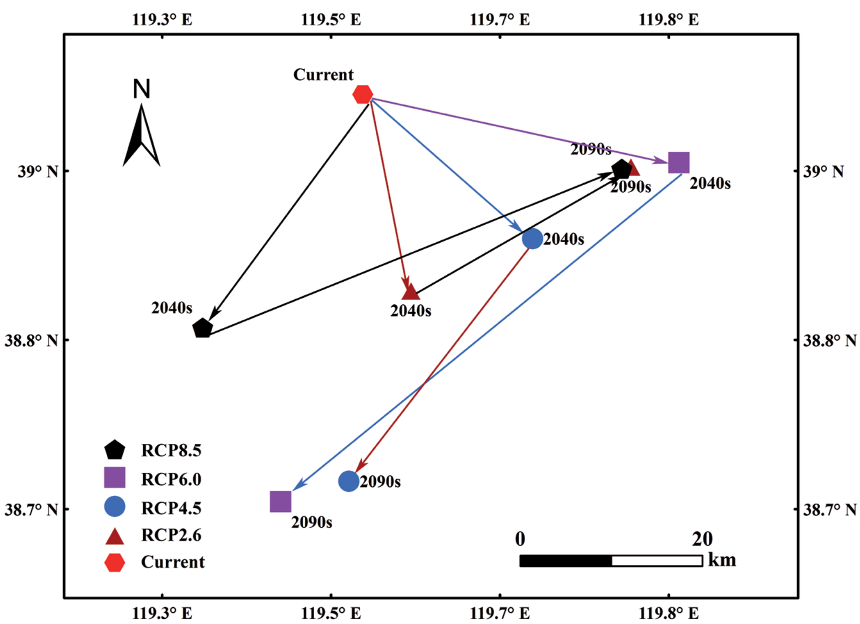

Fig. 12. Trajectory trend of the highly suitable habitat in the Bohai Sea.

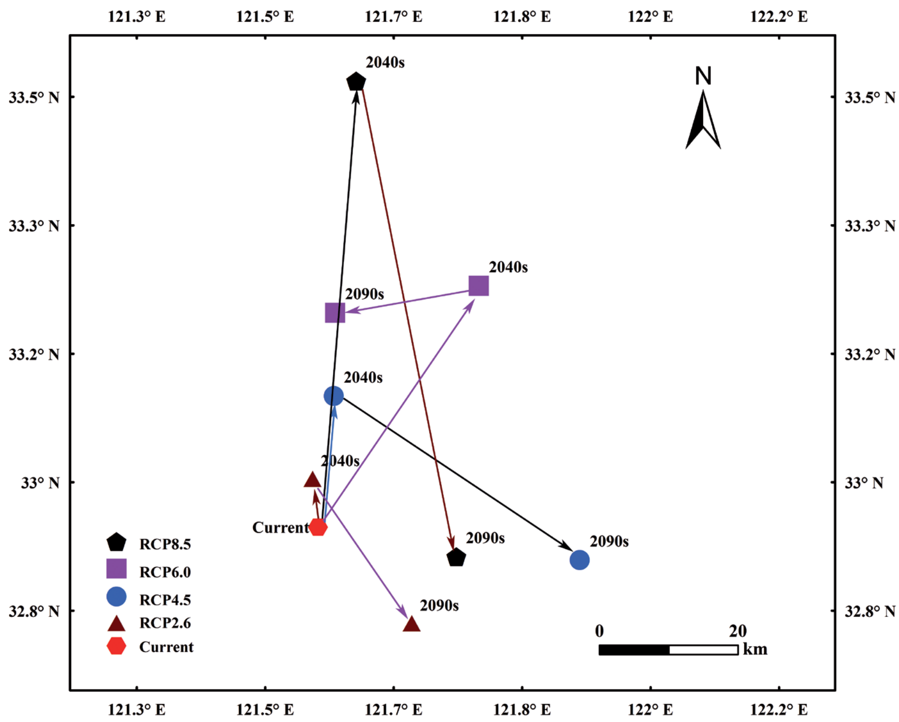

Fig. 13. Trajectory trend of the highly suitable habitat in the Yellow Sea.

then to the southwest by 34.45 km to 121.91°E/30.69°N (2090s). From current to 2090s, the centroid would generally moved 12.77 km to the northwest (Fig. 14). 2) Under RCP4.5, the centroid would move from 122.03°E/30.69°N (current) to the southeast by 11.43 km to 122.08°E/30.59°N (2040s), and then to the southwest by 11.39 km to 121.98°E/30.53°N (2090s). From current to 2090s, the centroid would generally moved 16.7 km to the southwest (Fig. 14). 3) Under RCP6.0, the centroid would move from 122.03°E/30.69°N (current) to the southwest by 31.71 km to 121.95°E/30.39°N (2040s), and then to the northwest by 20.06 km to 121.92°E/30.59°N (2090s). From current to 2090s, the centroid would generally moved 15.25 km to the southwest (Fig. 14).

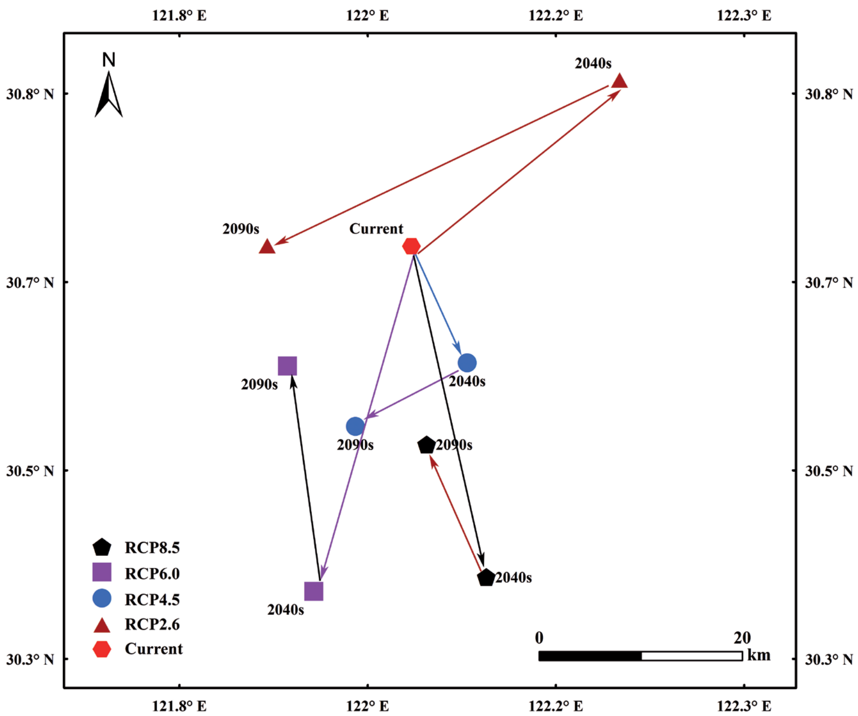

Fig. 14. Trajectory trend of the highly suitable habitat in the East China Sea.

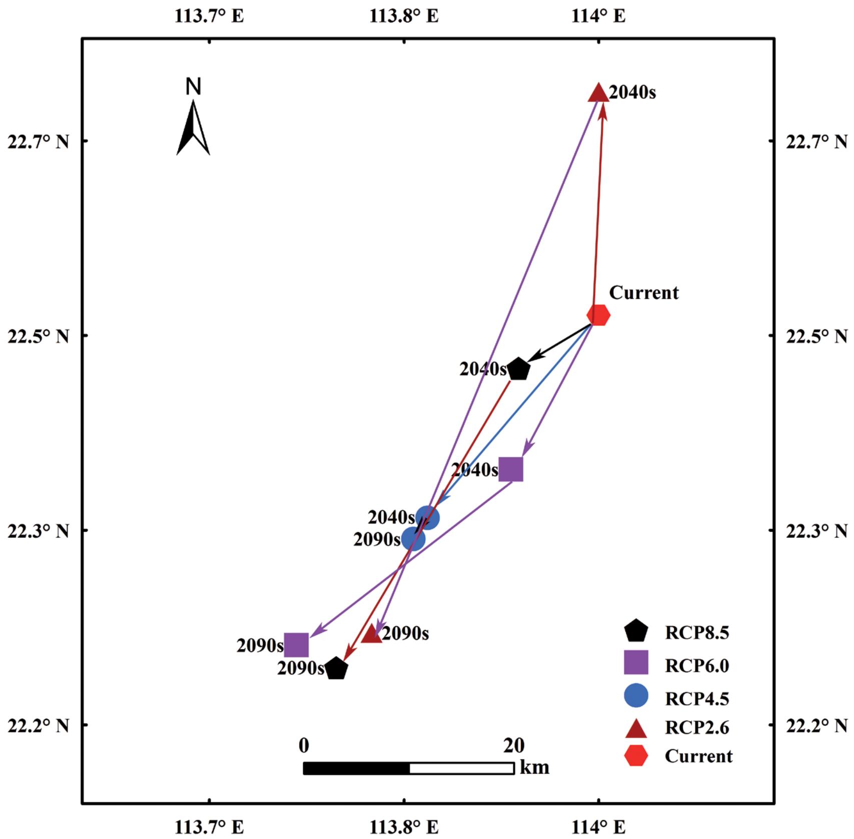

Fig. 15 Trajectory trend of the highly suitable habitat in the East China Sea.

4) Under SSP5-8.5, the centroid would move from 122.03°E/30.69°N (current) to the southeast by 30 km to 122.1°E/30.41°N (2040s), and then to the northwest by 12.86 km to 122.05°E/30.52°N (2090s). From current to 2090s, the centroid would generally moved 17.57 km to the southeast (Fig. 14).

Based on the centroid of the highly suitable habitat under the current and future climate change scenarios, the movement trajectory in the South China Sea was revealed as follows. 1) Under RCP2.6, the centroid would move from 114°E/22.51°N (current) to the north by 19.15 km to 114°E/22.71°N (2040s), and then to the southwest by 50.24 km to 113.81°E/22.25°N (2090s). From current to 2090s, the centroid would generally moved 33.41 km to the southwest (Fig. 15). 2) Under RCP4.5, the centroid would move from 114°E/22.51°N (current) to the southwest by 22.71 km to 113.85°E/22.34°N (2040s), and then to the southwest by 2.18 km to 113.84°E/22.33°N (2090s). From current to 2090s, the centroid would generally moved 24.86 km to the southwest (Fig. 15). 3) Under RCP6.0, the centroid would move from 114°E/22.51°N (current) to the southwest by 15.17 km to 113.92°E/22.38°N (2040s), and then to the southwest by 23.74 km to 113.74°E/22.23°N (2090s). From current to 2090s, the centroid would generally moved 38.29 km to the southwest (Fig. 15). 4) Under SSP5-8.5, the centroid would move from 114°E/22.51°N (current) to the southwest by 8.21 km to 113.93°E/22.47°N (2040s), and then to the southwest by 29.99 km to 113.77°E/22.21°N (2090s). From current to 2090s, the centroid would generally moved 37.6 km to the southwest (Fig. 15).

In this study, the migration trajectory of *Alexandrium* centroid was calculated, and it was found that the movement in the four sea areas was inconsistent, but it would move to the South as a whole. In the study of the centroid of species such as *Fritillaria cirrhosa* [47], *Blumea balsamifera* [20], *Isoetes* [21] and *Diaphorina citri* [48], it was found that with climate warming, species would migrate to regions at different latitudes. Because the population of *Alexandrium* is very large, the control of *Alexandrium* should not only refer to its potential suitable areas, but also consider topographic characteristics, climate change, ecosystem development and systematic geography, which is a greater challenge for the control of *Alexandrium* population in the 21st century.

Conclusions

The AUC values indicated that the MaxEnt model constructed in this study was very effective and feasible. The Jackknife test combined with the percent contribution rate showed that the Temperature. Range (bio24) was the most critical environmental variables affecting the geographical distribution of *Alexandrium*. By simulating the potential distribution in the four major sea areas of China and combining with field investigation, it was shown that special attention should be paid to the prevention and control of *Alexandrium* in the corresponding sea areas of Nantong, Yancheng, Ningbo, Jiaxing, Dongying, Binzhou, Cangzhou, Tianjin, Tangshan, Qinhuangdao, Shenzhen, Dongguan and Zhongshan. Under the future climate change scenarios, in the Bohai Sea and the East China Sea, the centriod of the highly suitable area would move to different latitudes and directions, move to the southeast in the Yellow Sea, and move to the southwest in the South China Sea.

Acknowledgments

This work was funded by the National Key Research Project (2017YFC1404601).

Data Availability

The datasets used and/or analyzed during the current study are available from the corresponding author on reasonable request.

Competing Interests

The authors declare no competing interests.

References

1. WANG Q., LIN L., CHEN X., WU W., WU H. Transportation of bloom forming species in ballast water by commercial vessels at Yangshan deep water port. Ocean Coast. Manag., **219**, 106045, **2022** 10.1016/j.ocecoaman.2022.106045.
2. KHALID N., AQEEL M., NOMAN A., HASHEM M., MOSTAFA Y.S., ALHAITHLOUL H.A.S., ALGHANEM S.M. Linking effects of microplastics to ecological impacts in marine environments. Chemosphere, **264**, 128541, **2021** 10.1016/j.chemosphere.2020.128541.
3. HESS-ERGA O., MORENO-ANDRÉS J., ENGER Ø., VADSTEIN O. Microorganisms in ballast water: Disinfection, community dynamics, and implications for management. Sci. Total Environ., **657**, 704, **2019** 10.1016/j.scitotenv.2018.12.004.
4. LEE J., HONG S., LEE J., CHOI T.S., RHIE K., KHIM J.S. Evaluation of residual toxicity of hypochlorite-treated water using bioluminescent microbes and microalgae: Implications for ballast water management. Ecotoxicol. Environ. Saf., **167**, 130, **2019** 10.1016/j.ecoenv.2018.10.002.
5. WERSCHKUN B., SOMMER Y., BANERJI S. Disinfection by-products in ballast water treatment: An evaluation of regulatory data. Water Res., **46**, 4884, **2012** 10.1016/j.watres.2012.05.034.
6. BAI M., TIAN Y., YU Y., ZHENG Q., ZHANG X., ZHENG W., ZHANG Z. Application of a hydroxyl-radical-based disinfection system for ballast water. Chemosphere, **208**, 541, **2018** 10.1016/j.chemosphere.2018.06.010.
7. DAVID M., LINDERS J., GOLLASCH S., DAVID J. Is the aquatic environment sufficiently protected from chemicals discharged with treated ballast water from vessels worldwide? – A decadal environmental perspective and risk assessment. Chemosphere, **207**, 590, **2018** 10.1016/j.chemosphere.2018.05.136.
8. RAK G., ZEC D., MARKOVČIĆ KOSTELAC M., JOKSIMOVIĆ D., GOLLASCH S., DAVID M. The implementation of the ballast water management convention in the Adriatic Sea through States' cooperation: The contribution of environmental law and institutions. Mar. Pollut. Bull., **147**, 245, **2019** 10.1016/j.marpolbul.2018.06.012.
9. LEWIS P.N., HEWITT C.L., RIDDLE M., MCMINN A. Marine introductions in the Southern Ocean: an unrecognised hazard to biodiversity. Mar. Pollut. Bull., **46**, 213, **2003** 10.1016/S0025-326X(02)00364-8.
10. KURNIAWAN S.B., PAMBUDI D.S.A., AHMAD M.M., ALFANDA B.D., IMRON M.F., ABDULLAH S.R.S. Ecological impacts of ballast water loading and discharge: insight into the toxicity and accumulation of disinfection by-products. Heliyon, **8**, e9107, **2022** 10.1016/j.heliyon.2022.e09107.
11. CHU K.H., TAM P.F., FUNG C.H., CHEN Q.C. A biological survey of ballast water in container ships entering Hong Kong. Hydrobiologia, **352**, 201, **1997** 10.1007/978-94-011-5234-1_20.
12. WANG Q., LIN L., CHEN X., WU W., WU H. Transportation of bloom forming species in ballast water by commercial vessels at Yangshan deep water port. Ocean & Coastal Management, **219**, 106045, **2022**.
13. WU H., SHEN C., WANG Q., RICHARD A.B., CHEN C. Survivorship characteristics and adaptive mechanisms of phytoplankton assemblages in ballast water. J. Oceanol. Limnol., **37**, 580, **2019** 10.1007/s00343-019-7288-9.
14. QIAN S.S., KENNEN J.G., MAY J., FREEMAN M.C., CUFFNEY T.F. Evaluating the impact of watershed development and climate change on stream ecosystems: A Bayesian network modeling approach. Water Research, **205**, 117685, **2021** https://doi.org/10.1016/j.watres.2021.117685.
15. CLERICI N., COTE-NAVARRO F., ESCOBEDO F.J., RUBIANO K., VILLEGAS J.C. Spatio-temporal and cumulative effects of land use-land cover and climate change on two ecosystem services in the Colombian Andes. Science of the Total Environment, **685**, 1181, **2019** https://doi.org/10.1016/j.scitotenv.2019.06.275.
16. ZARRINEH N., ABBASPOUR K.C., HOLZKÄMPER A. Integrated assessment of climate change impacts on multiple ecosystem services in Western Switzerland. Science of the Total Environment, **708**, 135212, **2020** https://doi.org/10.1016/j.scitotenv.2019.135212.
17. LEE C., SCHLEMME C., MURRAY J., UNSWORTH R. The cost of climate change: Ecosystem services and wildland fires. Ecological Economics, **116**, 261, **2015** https://doi.org/10.1016/j.ecolecon.2015.04.020.
18. CASAS-MONROY O., LINLEY R.D., CHAN P., KYDD J., VANDEN BYLLAARDT J., BAILEY S. Evaluating efficacy of filtration+UV-C radiation for ballast water treatment at different temperatures. Journal of Sea Research, **133**, 20, **2018** https://doi.org/10.1016/j.seares.2017.02.001.
19. REY T., FAUCHERRE N., VIRMOUX C., GALANO L. Paleoenvironmental reconstruction of the ancient harbors of King Louis IX (Aigues-Mortes, Rhone Delta, France).

Journal of Archaeological Science: Reports, **9**, 505, **2016** https://doi.org/10.1016/j.jasrep.2016.08.035.
20. GUAN L., YANG Y., JIANG P., MOU Q., GOU Y., ZHU X., XU Y.W., WANG R. Potential distribution of Blumea balsamifera in China using MaxEnt and the ex situ conservation based on its effective components and fresh leaf yield. Environ. Sci. Pollut. Res., **29**, 44003, **2022** 10.1007/s11356-022-18953-1.
21. YANG J., HUANG Y., JIANG X., CHEN H., LIU M., WANG R. Potential geographical distribution of the edangred plant Isoetes under human activities using MaxEnt and GARP. Glob. Ecol. Conserv., **38**, e2186, **2022** 10.1016/j.gecco.2022.e02186.
22. LIU L., WANG R.L., ZHANG Y.Y., MOU Q.Y., GOU Y.S., LIU K., HUANG N., OUYANG C.L., HU J.Y., DU, B.G. Simulation of potential suitable distribution of *Alnus cremastogyne* Burk. In China under climate change scenarios. Ecological Indicators, **133**, 108396, **2021**.
23. LI M.Y., ZHOU Q., HUANG W. Prediction of Potential Habitat for South China Tiger (Panthera tigris) Based on GIS and Web Datasets. Procedia Environmental Sciences, **10**, 1613, **2011** https://doi.org/10.1016/j.proenv.2011.09.255.
24. GUTIÉRREZ E.E., HEMING N.M., PENIDO G., DALPONTE J.C., LACERDA A.C.R., MORATELLI R., BUBADUÉ J.D.M., DA SILVA L.H., WOLF M.M., MARINHO-FILHO J. Climate change and its potential impact on the conservation of the Hoary Fox, Lycalopex vetulus (Mammalia: Canidae). Mammalian Biology, **98**, 91-101, **2019** https://doi.org/10.1016/j.mambio.2019.08.002.
25. GÜLÇIN D., ARSLAN E.S., ÖRÜCÜ Ö.K. Effects of climate change on the ecological niche of common hornbeam (Carpinus betulus L.). Ecological Informatics, **66**, 101478, **2021** https://doi.org/10.1016/j.ecoinf.2021.101478.
26. HEWER M.J., GOUGH W.A. Thirty years of assessing the impacts of climate change on outdoor recreation and tourism in Canada. Tourism Management Perspectives, **26**, 179, **2018** https://doi.org/10.1016/j.tmp.2017.07.003.
27. ZHAO S.D., XU N., LV S.H., WANG C.H. Dynamics of *Alexandrium* population and environmental factors in Daya Bay, the South China Sea. Ecologic Science, **25**, 109, **2006**.
28. YOU X.H. Studies on the growth of *Prorocentrum donghaiense* and *Alexandrium tamarense* under different environmental factor and the interspecific competition. M Type, Ocean University of China, Qingdao, **2006**.
29. LI B.X., YAO H.Q., SHEN X., LU X.P., LIANG Z.D., LIU F.L., ZHANG P.Y., WANG W.J. Potential geographic distribution of *Macrocystis pyrifera* in China based on MaxEnt model and ArcGIS. Progr. Fishery Sci., **2022** 10.19663/j.issn2095-9869.20211214002.
30. LI G.L., WANG W.J., LI B.X., YAO H.Q., SUN X., LIANG Z.D., LU X.P., LIU F.L. Potential geographic distribution of *Costaria costata* in China based on the MaxEnt Model and ArcGIS. Journal of Fishery Sciences of China, **28**, 1588, **2021**.
31. NORMA M., VOGLER R.E., MOLINA M.J., LLANO V.M., GRAHAM L. Potential distribution of the invasive freshwater dinoflagellate *Ceratium furcoides* (Levander) Langhans (Dinophyta) in South America. Journal of Phycology, **52**, 200, **2016**.
32. JAYASINGHE S.L., KUMAR L. Modeling the climate suitability of tea (*Camellia sinensis* (L.) O. Kuntze) in Sri Lanka in response to current and future climate change scenarios. Agricultural and Forest Meteorology, **272-273**, 102, **2019** https://doi.org/10.1016/j.agrformet.2019.03.025.
33. VESSELLA F., SCHIRONE B. Predicting potential distribution of Quercus suber in Italy based on ecological niche models: Conservation insights and reforestation involvements. Forest Ecology and Management, **304**, 150, **2013** https://doi.org/10.1016/j.foreco.2013.05.006.
34. KARIYAWASAM C.S., KUMAR L., RATNAYAKE S.S. Potential risks of invasive alien plant species on agriculture under climate change scenarios in Sri Lanka. Current Research in Environmental Sustainability, **3**, 100051, **2021** https://doi.org/10.1016/j.crsust.2021.100051.
35. SMITH C.L. The effects of climate change on the invasive alien plant Hypericum pseudohenryi in South Africa. South African Journal of Botany, **103**, 350, **2016** https://doi.org/10.1016/j.sajb.2016.02.174.
36. SAYIT H., NURRBAY A., XU Z.L., ARMAN J., SHAO H., VINIRA Y. Simulation of potential distribution patterns of the invasive plant species *Xanthium spinosum* L. (Bathurst burr) in Xinjiang under climate change. Acta Ecologica Sinica, **39**, 1551, **2019**.
37. CHEN J., WANG S.H., ZHU F., YUAN C.M. Risk evaluation of *Tithonia diversifolia* dispersal in Yunnan Province,China. Guihaia, **41**, 789, **2021**.
38. LI A., GAO M.M., CHEN X., LU T., LIU S.S. Distribution prediction of invasive species *Flaveria bidentis* in China: based on MaxEnt model and climate change scenario. Journal of Agriculture, **10**, 60, **2020**.
39. HABERKORN H., LAMBERT C., Le GOÏC N., QUÉRÉ C., BRUNEAU A., RISO R., AUFFRET M., SOUDANT P. Cellular and biochemical responses of the oyster Crassostrea gigas to controlled exposures to metals and Alexandrium minutum. Aquatic Toxicology, **147**, 158, **2014** https://doi.org/10.1016/j.aquatox.2013.12.012.
40. CHAPELLE A., LABRY C., SOURISSEAU M., LEBRETON C., YOUENOU A., CRASSOUS M.P. Alexandrium minutum growth controlled by phosphorus: An applied model. Journal of Marine Systems, **83**, 181, **2010** https://doi.org/10.1016/j.jmarsys.2010.05.012.
41. HIGO S., MAUNG-SAW-HTOO-THAW YAMATOGI T., ISHIDA N., HIRAE S., KOIKE K. Application of a pulse-amplitude-modulation (PAM) fluorometer reveals its usefulness and robustness in the prediction of Karenia mikimotoi blooms: A case study in Sasebo Bay, Nagasaki, Japan. Harmful Algae, **61**, 630, **2017** https://doi.org/10.1016/j.hal.2016.11.013.
42. HARRIS R.J., ARRINGTON D.A., PORTER D., LOVKO V. Documenting the duration and chlorophyll pigments of an allochthonous Karenia brevis bloom in the Loxahatchee River Estuary (LRE), Florida. Harmful Algae, **97**, 101851, **2020** https://doi.org/10.1016/j.hal.2020.101851.
43. LAMBERS J. Extinction risks from climate change. Science, **348**, 501, **2015**.
44. MESA T., POLO J., ARABIA A., CASELLES V., MUNNÉ-BOSCH, S. Differential physiological response to heat and cold stress of tomato plants and its implication on fruit quality. Journal of Plant Physiology, **268**, 153581, **2022** https://doi.org/10.1016/j.jplph.2021.153581.
45. LYU J., HE Q., CHEN Q., CHENG R., LI G., OTSUKI K., YAMANAKA N., DU S. Distinct transpiration characteristics of black locust plantations acclimated to semiarid and subhumid sites in the Loess Plateau, China. Agricultural Water Management, **262**, 107402, **2022** https://doi.org/10.1016/j.agwat.2021.107402.
46. LIU L., GUAN L.L., ZHAO H.X., HUANG Y., MOU Q.Y., LIU K., CHEN T.T., WANG X.Y., ZHANG Y., WEI B., HU J. Modeling habitat suitability of *Houttuynia cordata* Thunb (Ceercao) using MaxEnt under climate

change in China. Ecological Informatics, **63**, 101324, **2021**.

47. LIU L., ZHANG Y., HUANG Y., ZHANG J., MOU Q., QIU J., WANG R., LI Y., ZHANG D. Simulation of potential suitable distribution of original species of Fritillariae Cirrhosae Bulbus in China under climate change scenarios. Environ. Sci. Pollut. Res., **29**, 22237, **2022** 10.1007/s11356-021-17338-0.
48. WANG R.L., YANG H., WANG M.T., ZHANG Z., LI Q. Predictions of potential geographical distribution of Diaphorina citri (Kuwayama) in China under climate change scenarios. Scientific Reports, **10**, 1, **2020**.

Supplementary Material

Table S1. Distribution points of *Alexandrium*.

NO.	Longitude	Latitude	NO.	Longitude	Latitude
1	117.761	39.050	48	120.159	40.105
2	117.768	39.043	49	120.169	40.090
3	117.774	39.021	50	120.181	40.070
4	117.783	38.999	51	120.166	40.045
5	117.792	38.981	52	120.145	40.082
6	117.772	38.973	53	120.138	40.098
7	117.812	38.966	54	120.115	40.090
8	117.747	38.980	55	120.129	40.058
9	117.725	38.987	56	121.896	30.092
10	117.841	38.962	57	121.966	30.111
11	117.841	38.960	58	121.907	30.078
12	117.895	38.957	59	121.954	30.087
13	117.932	38.902	60	121.962	30.084
14	118.024	38.900	61	121.970	30.082
15	118.121	38.901	62	121.950	30.077
16	118.213	38.900	63	121.957	30.073
17	117.841	38.830	64	121.963	30.070
18	117.934	38.830	65	121.973	30.065
19	118.023	38.831	66	121.947	30.069
20	117.605	38.767	67	121.954	30.066
21	117.688	38.767	68	121.961	30.063
22	117.754	38.767	69	121.922	30.062
23	117.843	38.765	70	121.939	30.061
24	117.932	38.765	71	121.958	30.059
25	118.025	38.765	72	121.973	30.057
26	118.120	38.765	73	121.930	30.047
27	118.213	38.765	74	121.946	30.048
28	118.340	38.765	75	121.961	30.048
29	119.663	38.627	76	121.974	30.048
30	117.754	38.627	77	121.930	30.028

Table S1. Continued.

31	117.842	38.626	78	121.952	30.024
32	117.934	38.625	79	121.977	30.020
33	118.029	38.625	80	122.000	30.016
34	118.131	38.624	81	122.351	30.743
35	118.244	38.626	82	121.977	30.021
36	118.337	38.626	83	122.367	30.709
37	117.668	38.558	84	122.353	30.651
38	117.934	38.556	85	113.790	22.118
39	121.619	38.944	86	113.872	22.457
40	121.665	38.945	87	114.297	22.569
41	121.746	38.914	88	114.505	22.681
42	121.652	38.963	89	114.532	22.681
43	121.690	38.958	90	117.043	23.481
44	121.762	38.935	91	117.064	23.543
45	120.234	40.086	92	122.069	29.702
46	120.220	40.058	93	120.238	36.142
47	120.196	40.096	94	120.469	37.505

Table S2. Percent contribution and cumulative contribution of initial variables.

Variable	Percent contribution rate / %	Cumulative contribution rate / %
bio24	87.83	87.83
bio18	6.31	94.14
bio19	1.47	95.61
bio10	1.09	96.70
bio17	0.88	97.58
bio6	0.52	98.10
bio13	0.38	98.48
bio21	0.31	98.79
bio2	0.29	99.08
bio7	0.29	99.37
bio15	0.21	99.58
bio9	0.18	99.76
bio16	0.14	99.90
bio23	0.10	100.00

Table S3. Pairwise Pearson's correlation coefficients of climatic variables.

	bio2	bio6	bio7	bio9	bio10	bio13	bio15	bio16	bio17	bio18	bio19	bio21	bio23
bio6	0.91												
bio7	-0.38	-0.37											
bio9	-0.39	-0.38	1.00										
bio10	-0.36	-0.36	1.00	1.00									
bio13	0.55	0.68	0.24	0.22	0.25								
bio15	0.59	0.69	0.09	0.07	0.09	0.95							
bio16	0.08	0.28	0.54	0.54	0.55	0.87	0.76						
bio17	-0.33	-0.11	0.72	0.72	0.72	0.58	0.43	0.90					
bio18	0.80	0.64	-0.70	-0.70	-0.68	0.12	0.32	-0.37	-0.72	1.00			
bio19	0.38	0.39	-0.18	-0.18	-0.18	0.47	0.72	0.27	0.00	0.55			
bio21	0.34	0.37	-0.19	-0.19	-0.19	0.45	0.70	0.26	0.01	0.53	1.00		
bio23	0.98	0.89	-0.50	-0.52	-0.49	0.45	0.49	-0.04	-0.44	0.84	0.32	0.29	
bio24	-0.61	-0.50	0.30	0.31	0.28	-0.05	0.11	0.24	0.39	-0.33	0.49	0.53	-0.66